Photoproduction of Positive Pions in Hydrogen-Counter Telescope Method*

A. V. TOLLESTRUP, J. C. KECK, AND R. M. WORLOCK
California Institute of Technology, Pasadena, California
(Received March 7, 1955)

The excitation functions for positive pion production from hydrogen have been obtained in the energy region from 230 Mev to 450 Mev and at laboratory pion angles of 24°, 38°, 53°, 73°, 93°, 115°, 140°, and 160°. The pions are detected and identified by measuring their range and ionization in a scintillation counter telescope. The above data are analyzed to give the angular distributions in the center-of-momentum system, and a least-squares analysis made to determine coefficients in $\sigma(\theta)=A+B\cos\theta+C\cos^2\theta$. The total cross section shows a peak at 300 Mev of magnitude 2.20×10^{-28} cm². The coefficient B passes through a maximum negative value at 250 Mev and then passes through zero at 325 Mev and remains positive up to the highest energy measured.

I. INTRODUCTION

THE operation of the CalTech synchrotron has made it possible to obtain data on the photoproduction of positive mesons from hydrogen in the energy region from 200 Mev to 500 Mev and thus considerably extend the region over which the cross section has been measured. The measurements reported here consist of excitation curves at pion angles of 24°, 38°, 53°, 73°, 93°, 115°, 138°, 160° in the laboratory system and from these curves the angular distributions in the c.m. system at photon energies of 230, 260, 290, 320, 350, 380, 410, 440, and 470 Mev are derived. Previous measurements of this process[1] have been done at 300 Mev and below and have left undecided the question as to whether or not the $T=\frac{3}{2}$, $J=\frac{3}{2}$ state plays a predominant role in the photoproduction as predicted by strong coupling theory.[2]

At the time this experimental program was undertaken it was realized that it would be possible to perform the measurements by either of two methods. In both methods the incident photon energy must be calculated from a knowledge of the pion energy and the dynamics of the reaction studied. This energy can be inferred either by measuring the pion range in a scintillation counter telescope or by measuring the pion momentum by means of deflecting magnets.[3] The second method is described in the preceding paper and is hereafter referred to as the "magnet method." These two techniques are subject to quite different systematic errors and tend to complement each other. For instance, the magnet method at low energies required corrections for slit edge scattering and penetration and also rather large decay corrections due to the long flight path traversed by the mesons. The telescope was subject to these effects only to a very limited extent, and at low energies all of the corrections to the data were small and amenable to exact calculation. However, at high energy the telescope method suffers from rather big corrections due to the large interaction of the pions with the material in which their range is being measured. The final results of the two experiments do not agree in complete detail, and tend to indicate that undetected systematic errors still exist in either or both of the experiments. These details will be discussed further at the end of the paper. On the other hand, the agreement between the experiments is such that no doubt is left about the over-all behavior of the process and a good comparison with existing theories is possible.

II. EXPERIMENTAL METHOD

(a) Collimation

The bremsstrahlung beam from an internal 0.016-in. thick strip of copper is first collimated by a $\frac{1}{2}$-in. hole in a 12-in. thick lead block located 12 ft from the copper target. This primary collimation is followed by two secondary collimators which are of such a size and aligned in such a way that they do not intercept the direct beam. One of these secondary collimators is located in a concrete wall which shields the experimental area from the machine and the final one is just in front of the high pressure hydrogen target and arranged so as to shield the walls of the steel target cylinder from x-rays, as shown in Fig. 1. The beam at the target is $1\frac{1}{2}$ in. in diameter.

(b) Target

The high-pressure hydrogen target is a steel cylinder 17 in. long by 2 in. in diameter which is filled with gas to a pressure of 2000 lb and cooled to a liquid nitrogen temperature. The walls of the target, through which the mesons had to pass, consisted of 0.030 in. of steel and $1\frac{1}{2}$ in. styrofoam insulation. The loss of energy experienced by the mesons in passing through the gas and the target wall was taken into account when computing the range of the meson. The temperature was measured at the two ends of the target by means of thermocouples and the average value was used in com-

* This work was supported in part by the U. S. Atomic Energy Commission.
[1] J. Steinberger and A. S. Bishop, Phys. Rev. **86**, 171 (1952); White, Jacobson, and Shalz, Phys. Rev. **88**, 836 (1952); Jarmie, Repp, and White, Phys. Rev. **91**, 1023 (1953); Jenkins, Luckey Palfrey, and Wilson, Phys. Rev. **95**, 179 (1954); White, Jakobson, and Repp, Bull. Am. Phys. Soc. **29**, No. 8, 21 (1954).
[2] K. Brueckner and K. M. Watson, Phys. Rev. **86**, 928 (1952).
[3] Walker, Teasdale, Peterson, and Vette, preceding paper [Phys. Rev. **99**, 210 (1955)].

puting the density.[4] Generally, a value of about 0.03 g/cm^3 was obtained with an accuracy of ± 3 percent.

(c) Monitor

The monitor was a thick ionization chamber and the problem of its calibration is described in reference 3.

(d) Detector

The bremsstrahlung beam striking the hydrogen target produced a cylindrical source of mesons. The detector first had to identify the particle counted as a meson and secondly define its angle and energy in order that the energy of the photon producing the meson could be calculated from the dynamics of the reaction. Figure 1 shows how this was accomplished. The four scintillation counters numbered from 1 to 4 are connected in such a way that a particle producing a pulse simultaneously in C_1, C_2, C_3, but not in C_4 has its pulse height measured in C_2. A_1, A_2, and A_3 are blocks of copper of adjustable thickness and hence only those particles were accepted which had a range between $R=C_1+A_1+C_2+A_2$ and $R+\Delta R=C_1+A_1+C_2+A_2+C_3+A_3$. The energy was then deduced from the range-energy curves for mesons in copper.[5] The number

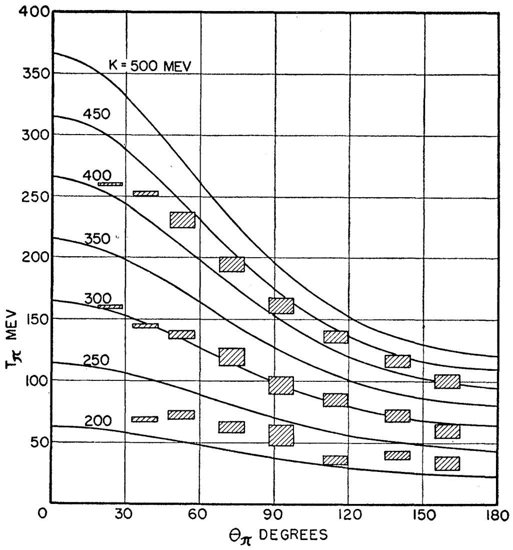

FIG. 2. Kinematics of charged pion production. The shaded areas indicate resolution of the telescope at typical points. The width of a rectangle is the half-width of the telescope angular resolution function and the height is the pion energy interval accepted.

of photons contributing to the reaction is then given by

$$N(\gamma)=N(k)\Delta k=N(k)\frac{\partial k}{\partial E_\pi}\frac{\partial E_\pi}{\partial R}\Delta R, \tag{1}$$

where $N(k)$ = number of photons/Mev in the bremsstrahlung spectrum.

The angular resolution function was triangular in shape with a width at half-maximum of $\Delta\theta=a/l$, where a was the width of counters C_1 and C_3 and l is their spacing. Thus 75 percent of the counts occur within this half-angle which in general was about 10°. Figure 2 shows a summary of this information. The graph is one of the T_π *vs* θ_π in the laboratory for various fixed photon energies. Since the telescope defines a ΔT_π and a $\Delta\theta_\pi$ as indicated above, rectangles ΔT_π high by $\Delta\theta_\pi/2$ wide may be plotted on a $T_\pi-\theta_\pi$ graph representing the resolution of the telescope. A few representative rectangles are shown in Fig. 2 from which it may be seen that the photon energy interval accepted was 25 Mev or less.

The number of mesons counted by the telescope per coulomb collected on the beam integrator is given by the expression

$$N_\pi(\theta)=N_{\mathrm{H}}N(k)\Delta k\int_{\Omega\tau}\frac{d\sigma}{d\Omega_{\mathrm{lab}}}d\Omega d\tau, \tag{2}$$

where N_{H} is the number of hydrogen atoms per cm^3, $N(k)$ is the number of photons of energy k per Mev per coulomb collected on the ion chamber, and the integral is over the coordinates describing the counter and the volume of the target. It is possible to carry this integral out exactly, but it has been found more convenient to

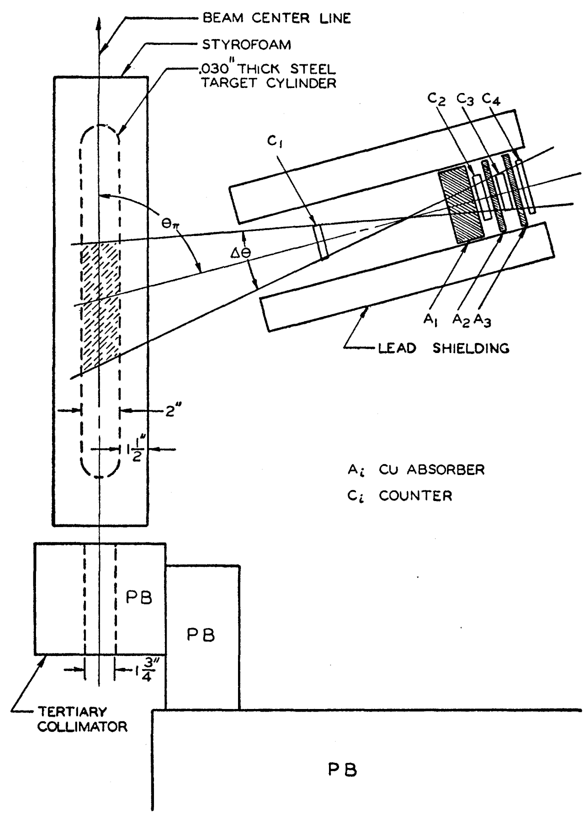

FIG. 1. Plan view of target and telescope.

[4] Johnston, Bezman, Rubin, Swanson, Corak, and Rifkin, U. S. Atomic Energy Commission Report MDDC-850 (unpublished).
[5] Aron, Hoffman, and Williams, U. S. Atomic Energy Commission Report AECU-663 (unpublished).

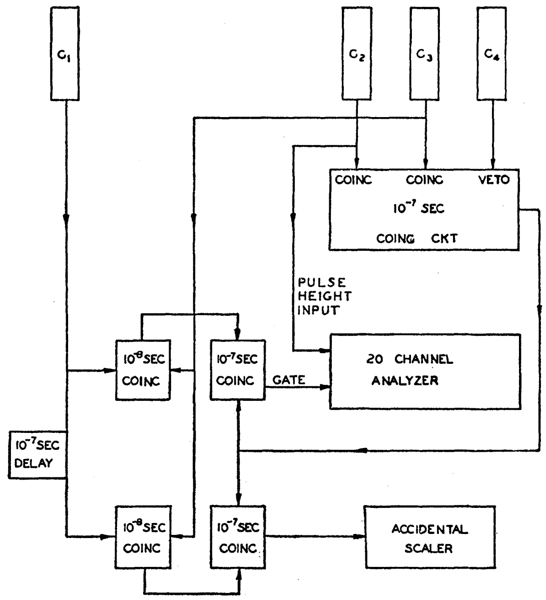

FIG. 3. Block diagram of electronics for 4-counter telescope.

use a series expansion:

$$N_\pi(\theta)=\frac{N_{\mathrm{H}}a^2hN(k)\Delta k}{lc\sin\theta}(1+\alpha+\cdots)\frac{d\sigma(\theta)}{d\Omega_{\mathrm{lab}}}. \tag{3}$$

Here a is the width of the counters C_1 and C_3, h is the height of counter C_3, c the distance from the center of C_3 to the point where the axis of the telescope intersects the beam axis, and l is the distance from C_1 to C_3. The term α involves the squares of the ratios of beam radius, h, and a to the distance c. These terms have been calculated and amount to 0.5 percent for θ equal to 160° and are smaller at other angles.

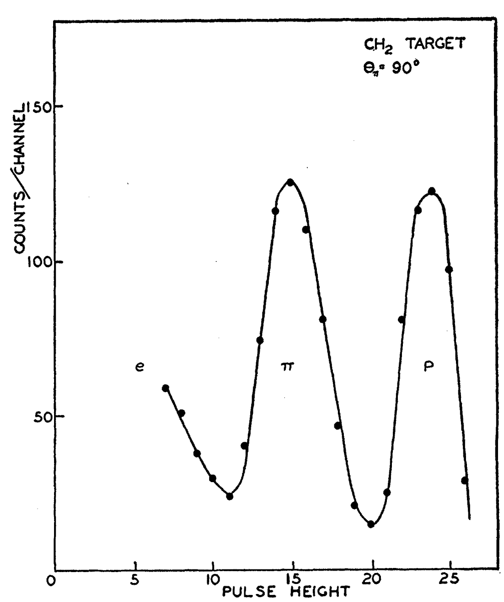

FIG. 4. Pulse-height spectrum from CH_2 target at lab angle of 90°, showing peaks due to electrons, mesons, and protons.

In the course of the experiment three different telescope arrangements were used. The first had the electronics arranged as shown in a block diagram in Fig. 3. The counters are numbered as in Fig. 2. The pulses from counters C_1 and C_3 were put into a fast coincidence circuit with a resolving time of 10^{-8} sec. These counters defined the solid angle and in addition the presence of C_1 made the telescope insensitive to γ rays converted by the copper absorbers which were placed between C_1 and C_2. If in addition to a fast coincidence between C_1 and C_3 a slow coincidence was recorded between C_2 and C_3, then the gate to the 20-channel pulse-height analyzer was opened and the pulse height in counter C_2 was recorded. A typical pulse-height spectrum from a CH_2 target is shown in Fig. 4 and it is seen that the three peaks representing electrons, π mesons, and protons are easily resolved. Figure 5 shows typical results obtained from the hydrogen target at 73° for three different photon energies. It is seen that in addition to the π mesons, there is a peak due to electrons and a small peak due to protons. By varying absorbers A_1 and A_2 it was shown that the source of the proton peak was due to π mesons which made a star in absorber A_1 after triggering counter C_1. A proton from this star would then trigger counters C_2 and C_3.

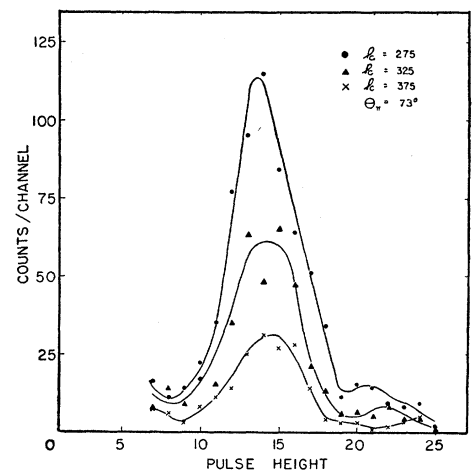

FIG. 5. Pulse-height spectra at pion lab angle of 73° and photon energies of 275, 325, and 375 Mev obtained with the 4-counter telescope.

The telescope could be triggered also by various accidental events. The most serious of these was caused by a meson which did not pass through C_1, but did actuate C_2 and C_3 properly and was also accidentally coincident with a pulse in C_1. To provide information for correction of this type of event, an accidental channel was constructed by sending the delayed pulses from C_1 through electronic circuits identical with those through which the nondelayed pulses traveled. The accidental channel was then aligned in such a way that it had the same counting rate as the true channel when both channels received delayed pulses from C_1. The continuous monitoring of the accidental events not only provided the data for the necessary corrections, but also enabled one to adjust the experimental conditions such that the corrections never became large.

At the forward angles of 24° and 38° the structure of the telescope was modified. At these angles C_1, which must be biased to count minimum ionization particles, counted at an excessive rate due to electrons produced in the ends of the bomb and scattered into the telescope. Hence, counter C_1 was replaced by wolfram slits and these slits in conjunction with counter C_3 then defined the angular acceptance of the telescope. In addition, a $\pi-\mu$ decay scheme was constructed to help identify the mesons. The block diagram of the

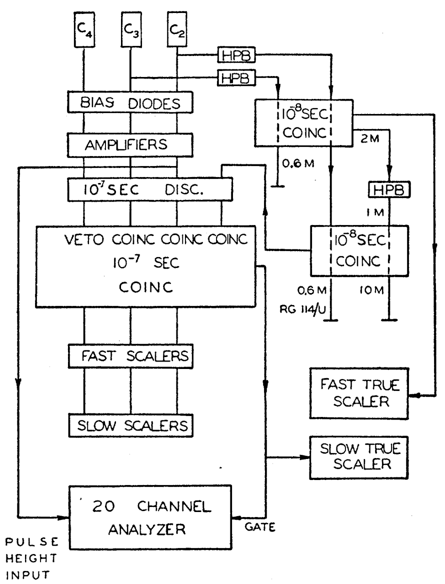

FIG. 6. Block diagram of electronics in $\pi-\mu$ decay detection scheme. Cable length in meters. HPB indicates a Hewlett Packard 460-B amplifier.

electronics is shown in Fig. 6. It may be seen that a fast coincidence was required between counters C_2 and C_3. This coincidence pulse was then formed into a gate signal 0.1 μsec in duration and delayed by about 15 m μsec and then put into coincidence with any delayed pulse from counter C_3. This, it should be noted, reduced the detection efficiency, since only the μ mesons falling in the delay interval were detected. The copper absorber A_3 was removed and a special 1-in. thick counter built for C_3 which then defined the ΔR of the telescope. The output of this second fast coincidence circuit was then combined with the slower electronics to gate the pulse-height analyzer on counter C_2. Thus, not only was a $\pi-\mu$ decay required, but the dE/dx of the particle was also measured in counter C_2. Figure 7 shows the pulse-height spectrum recorded in counter C_2. The complete lack of peaks corresponding to electrons

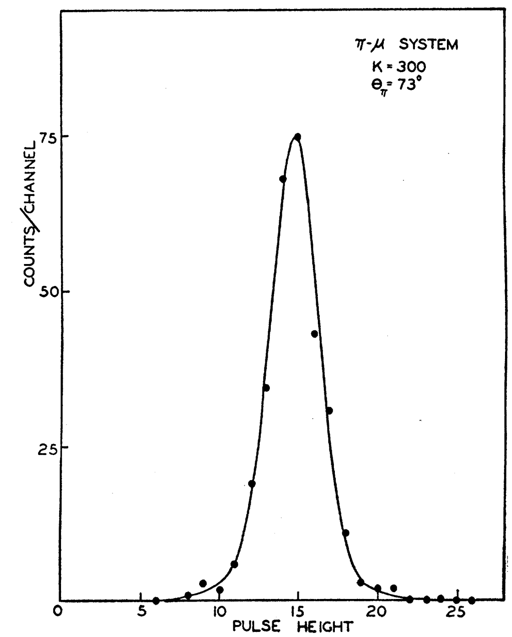

FIG. 7. Pulse-height spectrum at pion lab angle of 73°, and photon energy of 300 Mev using $\pi-\mu$ decay identification system. Electrons would have fallen in the interval between 0 and 10 and protons between 20 and 25 on the pulse-height scale.

or protons indicates the system was identifying π mesons in a very satisfactory fashion. The efficiency of this system was then obtained by calibrating it against the previous telescope at 73° and 300 Mev. The statistical accuracy of this calibration was (±3 percent).

At 38° the excitation curve obtained with the $\pi-\mu$ telescope was 20 percent higher than with the other telescope at energies above 300 Mev and even higher than this at lower energies. A check at 53° did not display this effect and it is felt that here the counting rates were low enough so that the first telescope was operating properly. The counting rates obtained with the $\pi-\mu$ method were only about a sixth those that could have been obtained by the previous system because of the small ΔR which the 1-in. liquid cell presented and also because of the reduced efficiency of detecting the μ-decay pulse. This resulted in larger statistical errors in the data at these two angles.

Finally, the 160° data were obtained at a considerably later time than the rest of the data. This was due in part to the necessity of turning the hydrogen target end for end in order to reach this extreme angle with the counters. In the meantime, the telescope was rebuilt with plastic scintillators in place of the previous liquid cells. When the telescope was reassembled, wolfram slits were placed in front of counter C_1 and thus the slits and counter C_3 defined the angular acceptance of the telescope. The excitation curve was then run at 160°, and as a check the 73°, 115°, and 140° curves were re-run. When the data were reduced, it was discovered that they produced results 20 percent higher than were

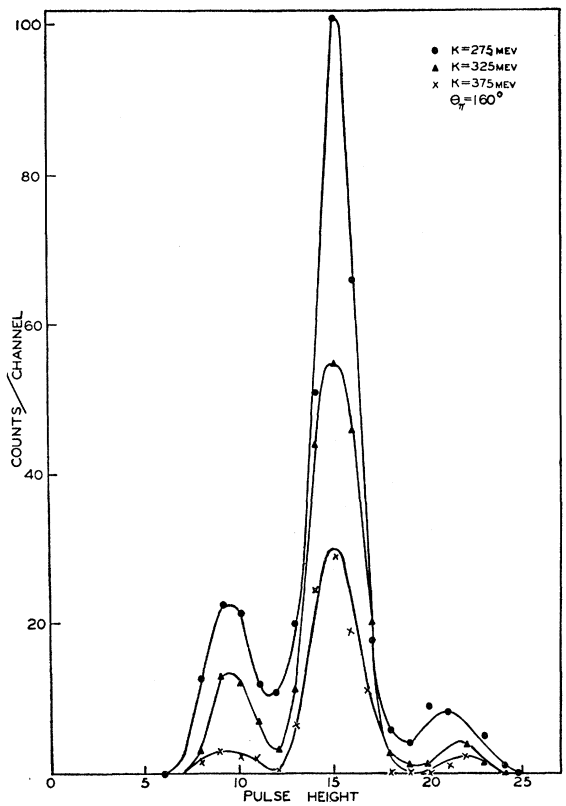

FIG. 8. Pulse-height spectra obtained at pion lab angle of 160° and photon energies of 275, 325, and 375 Mev.

previously obtained. Calculations indicated that scattering and slit-edge penetration could account for only half of this effect. However, it was felt that there were other systematic errors in the absolute value of these data and consequently the data at 73°, 115°, and 140° were compared with the previous data to obtain a normalization factor for the 160° results. A least-square analysis was made to obtain the normalizing constant, and gave 0.820±0.013. The new data, when thus normalized and plotted, interlaced the old data nicely and showed no indication of systematic deviations in either energy or angle. Figure 8 shows typical pulse-height curves obtained in counter C_2 at 160° for three different photon energies.

III. RESULTS

The differential cross sections in the laboratory system *vs* photon energy obtained in the manner described above are shown in Figs. 9 through 12. The data at 38° and 24° are statistically not as accurate as the data at other angles because of the calibration required by the $\pi-\mu$ telescope and also because of the low counting rates obtained by the $\pi-\mu$ method.

Angular distributions in the center-of-mass system at 30-Mev intervals of photon energy were plotted from the excitation curves by using either the actual data or approximations to these data rather than the smoothed curves. These angular distributions were then fitted to the form

$$d\sigma/d\Omega = A + B\cos\theta + C\cos^2\theta, \tag{4}$$

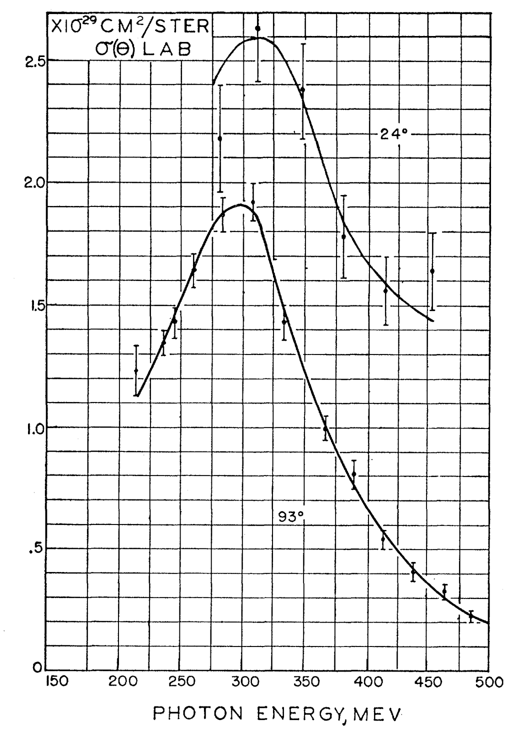

FIG. 9. Laboratory cross section as function of incident photon energy at pion lab angles of 24° and 93°.

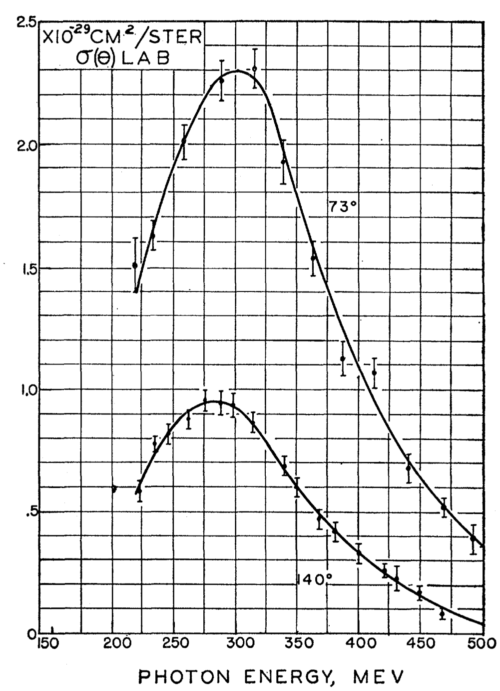

FIG. 10. Laboratory cross section as function of incident photon energy at pion lab angles of 73° and 140°.

by means of a least-squares analysis. The weighting of the input data in this analysis included both statistical errors plus estimates of those systematic errors that effect the relative values of the input data. The results of this analysis are shown in Figs. 13 to 15 where the solid curves are calculated from Eq. (4) using the least squares values for A, B, and C. A plot of these coefficients *versus* energy is shown in Fig. 16 and their values at 30-Mev intervals are listed in Table I. The total cross section curve is shown in Fig. 17 as computed from

$$\sigma(k)=4\pi(A+C/3), \tag{5}$$

and values are listed in Table I.

IV. DATA CORRECTION

(a) Absorption Correction

The largest correction to the data was due to absorption of the π mesons in the copper stopping material of the telescope. For instance, at 73°, 300-Mev photon energy 32 percent of the incident mesons interacted in the copper before coming to rest and at 24°, 450-Mev photon energy this number increased to 77 percent. Although this correction is rather large, it can be accurately made if the value of the mean free path of mesons in copper is known. The measurement of the π^- interaction cross section in copper has been made at 85 Mev[6] as well as 113 and 137 Mev.[7] Since the measurements all agree within the accuracy of the experi-

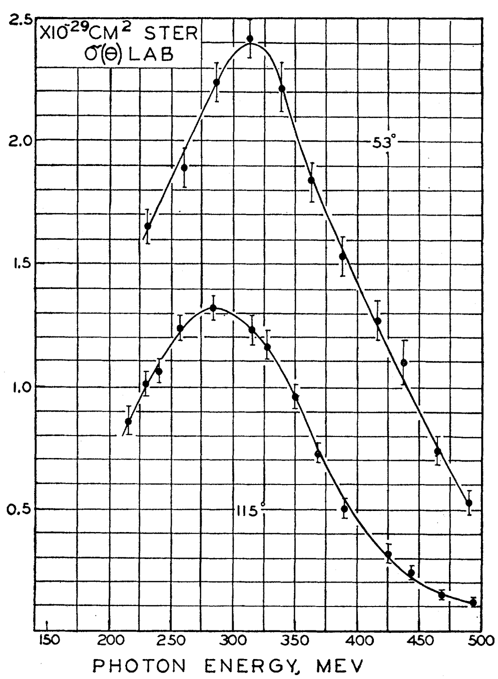

FIG. 11. Laboratory cross section as function of incident photon energy at pion lab angles of 53° and 115°.

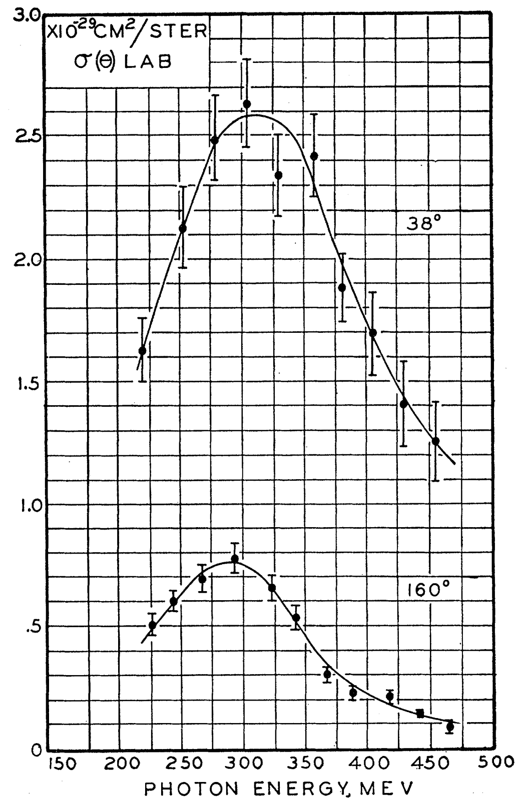

FIG. 12. Laboratory cross section as function of incident photon energy at pion lab angles of 38° and 160°.

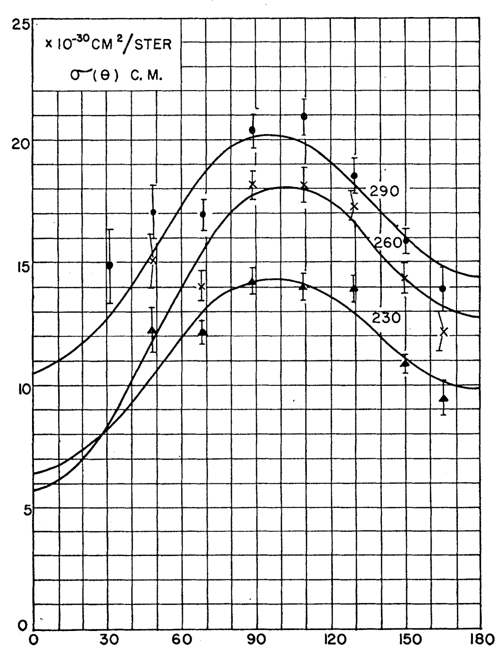

FIG. 13. Angular distribution curves in c.m. system for 230-, 260-, and 290-Mev incident photon energies. Solid curves are the least-square fit.

[6] Chedester, Isaacs, Sachs, and Steinberger, Phys. Rev. **82**, 958 (1951).

[7] R. L. Martin, Phys. Rev. **87**, 1052 (1952).

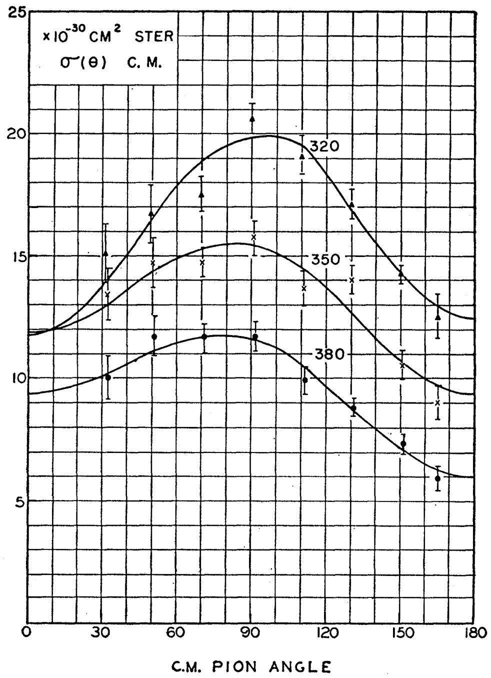

FIG. 14. Angular distribution curves in c.m. system for 320-' 350-, and 380-Mev incident photon energies. Solid curves are the least-square fit.

ments, we have used a weighted average for the mean free path of 12.1 cm with an uncertainty of 5 percent. The maximum uncertainty in the absorption correction amounts to 7 percent at 24° and 450 Mev and is reduced to 2.5 percent at 300 Mev and 73°.

(b) Scattering in the Absorbers

The effect of multiple scattering and shadow scattering in the absorbers was calculated and a correction made to the data. This amounted to less than 3 percent. Scattering in the lead shielding surrounding the telescope was calculated and found to be negligible. Scattering corrections in the bomb wall and in the front counter, when used, were assumed to be negligible due to the fact that scattering into the telescope tends to cancel scattering out of the telescope. To test this hypothesis absorber was shifted from position A_1 to a position in front of counter C_1. No effect could be detected up to $\frac{7}{16}$ in. of copper at a meson energy of 65 Mev. This was an excellent test since the amount of scattering material was always much less than this amount.

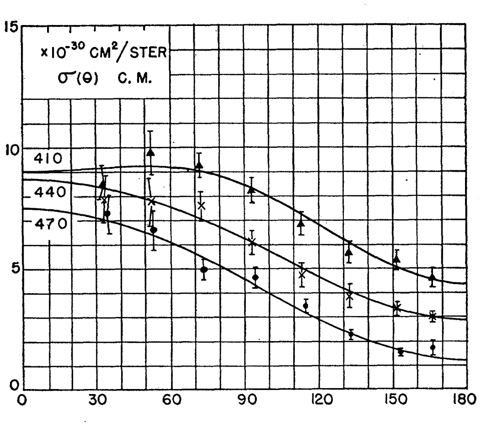

FIG. 15. Angular distribution curves in c.m. system for 410-, 440-, and 470-Mev incident photon energies. Solid curves are the least-square fit.

(c) Range Energy Relation

Meson ranges in copper were obtained from the proton range energy relation given by Aron.[5] These ranges were corrected for multiple scattering in the absorbers in order to obtain the projected ranges which the telescope measures. This effect amounts to a shortening of the meson range in copper as calculated from Aron's curves by about 1.5 percent. The ranges were assumed to be accurate to 1 percent +0.01 cm.

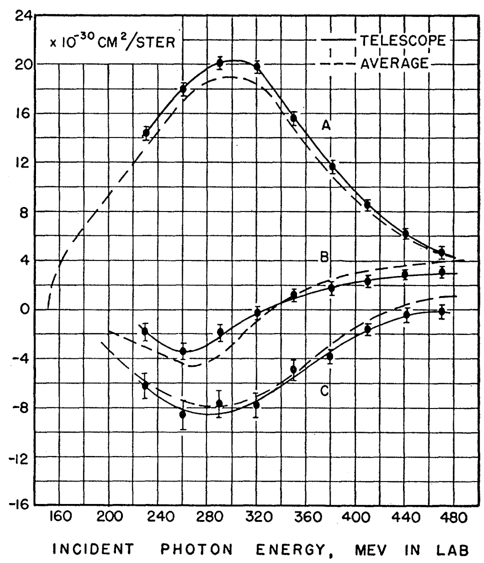

FIG. 16. Angular distribution coefficients. The solid curves represent the results of this experiment. The dotted curves are the average of all experiments as obtained in reference 3.

(d) ΔR Determination

The range of photon energies effective in producing mesons which actuated the telescope was, as indicated above, directly proportional to the ΔR of the telescope which in turn was made up of absorber A_3 plus counter 3. As a check, the equivalent thickness in centimeters of copper of C_3 was experimentally measured in the following manner. The counts in the meson peak were observed as absorber A_3 was varied from 0 up to $\frac{1}{4}$ in. of copper in 5 steps while adjusting absorber A_2 to keep the mean range constant. The data when plotted should give a straight line which has an intercept with the absorber A_3 axis equal to the equivalent thickness of counter 3. The results are shown in Fig. 18 where a least-squares fit to the data has been made. The equivalent thickness of the counter thus measured is 0.285±0.015 cm copper, whereas the calculated value was 0.275 which is equal to the measured value within the statistical accuracy of the experiment. Since ΔR was composed of the counter plus the absorber A_3, the error is less than the statistical uncertainty of the above experiment and was given the value of ±2 percent.

(e) Accidentals and Dead-Time Correction

As has been described above, the accidental events were monitored simultaneously with the real events by means of delayed channels. This correction amounted to less than 5 percent in general, but in a few exceptional cases rose to 15 percent. In addition a few counts were missed because of dead-time losses caused by the veto counter C_4 being accidentally triggered in coincidence with a true event. This effect was corrected for and amounted to less than 3 percent in general, but again in a few cases got as high as 15 percent.

TABLE I. Results obtained by a least-squares determination of the coefficients A, B, and C in Eq. (4) of the text. Also in the last column is listed the total cross section as computed from Eq. (5).

k (Mev)	A	B (units 10^{-29} cm²/sterad)	C	Total
230	1.43 ±0.03	−0.167±0.058	−0.619±0.095	15.30±0.33
260	1.79 ±0.04	−0.348±0.073	−0.862±0.120	18.80±0.40
290	2.02 ±0.04	−0.183±0.061	−0.768±0.110	22.05±0.38
320	1.99 ±0.04	−0.035±0.056	−0.782±0.095	21.70±0.36
350	1.55 ±0.04	+0.122±0.051	−0.489±0.089	17.43±0.34
380	1.16 ±0.03	+0.172±0.042	−0.388±0.074	12.90±0.30
410	0.85 ±0.026	+0.232±0.037	−0.176±0.059	9.89±0.26
440	0.625±0.031	+0.292±0.042	−0.042±0.062	7.64±0.29
470	0.461±0.021	+0.311±0.037	−0.022±0.050	5.68±0.24

The veto counter had an additional effect for which it was necessary to correct. A valid count was discarded when the π meson correctly triggered the telescope, but then the resulting decay electron activated the veto counter within the resolving time of the slow coincident circuits. This effect has been calculated to be 6 percent ±2 percent.

(f) Backgrounds

The backgrounds were obtained with the target empty and typically were less than 10 percent, but sometimes as high as 30 percent of the counts from the gas. The geometry of the telescope was always such that the steel ends of the target were excluded from the region contributing counts to the telescope.

V. ERRORS

A summary of the assumed errors is given below. These are divided into two classes. The first are errors which are independent of energy and angle and hence affect the absolute value of all the results. These errors are not included in the results shown on any of the graphs or in the results quoted in Table I.

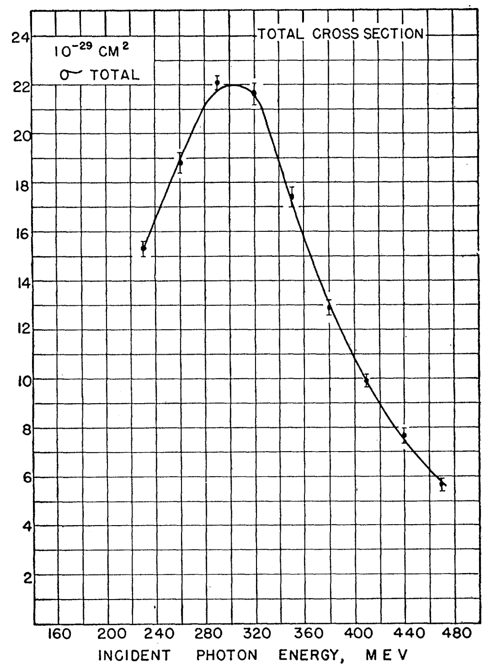

FIG. 17. Total cross section, for $\gamma+p\rightarrow\pi^++n$.

They are the following:

(1) Beam calibration: 7 percent.
(2) H_2 gas density: 3 percent.
(3) ΔR: 2 percent.
(4) Solid angle: 2 percent.
(5) μ decay actuating veto counter: 2 percent.

The combination of the above yields 8 percent as the error in absolute cross section.

In addition to the above, there exists both systematic errors which vary with angle as well as the random statistical errors. These errors were combined into a weighting factor which varied from point to point when the least squares fit of the angular distributions were made, and this is the error shown on the curves for the

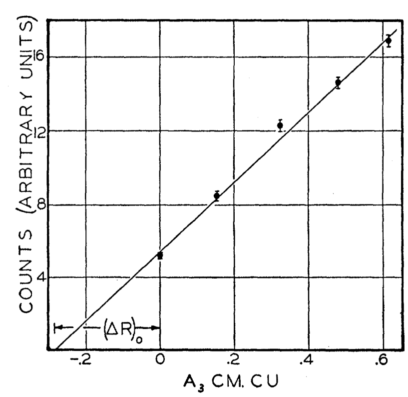

FIG. 18. Counting rate as function of absorber A_3. The line represents the least-square fit to the points. The intercept with the abscissa gives the equivalent thickness of counter C_3.

coefficients A, B, C, and given in Table I. These weighting factors were composed from the following errors:

(1) Statistical errors in the number of counts recorded.

(2) Error in absorption correction: uncertainty in mean free path equal to 5 percent.

(3) Errors in range-energy relations in copper: 1 percent +0.01 cm.

(4) Error in telescope angle: 0.7°.

(5) Day-to-day random errors in beam calibration, gas density, etc: 2 percent.

(6) Statistical factor in calibration of the telescope at 24°, 38°, and 160°.

(7) Errors in resolving the meson peaks from the electron and proton peaks: 2 percent.

VI. DISCUSSION OF RESULTS

A comparison of this experiment with other experiments may be made by examining Fig. 16. The dotted curve was obtained by an attempt to average all of the data available from Cornell, Illinois, and CalTech. These data are shown in Fig. 15 of the preceding paper.[3] In the energy region considered in this paper the dotted curve is essentially an average of the telescope results and the magnet results. Therefore the difference between the two experiments is about double the difference between the two curves of Fig. 16. It is seen that there is a reasonable agreement between this experiment and the magnet experiment on the A and C coefficients, but that there is quite a disagreement on the B coefficient. This shows up in a detailed comparison of the angular distribution curves where it is found that the magnet method gives results that are high compared to the telescope for either forward angles at photon energies higher than 380 Mev or backward angles at energies in the neighborhood of 290 Mev. In the region of $\theta_{\text{c.m.}}$ equal to 90°, the experiments agree quite well with each other and also with the Cornell and Illinois results at lower energy.

As has been pointed out, the telescope data are subject to large absorption corrections at high energies, whereas the magnet method does not suffer from this uncertainty. The fact that the cross sections agree quite well at 73° up to 450-Mev photon energy would seem to indicate that we make this correction accurately up to a meson energy of 200 Mev. This disagreement at forward angles involving meson energies higher than this cannot be due to errors in the absorption correction. This is because a pion interaction cross section in copper of twice geometrical would have to be used in order to make the two experiments agree in this region. In the backward hemisphere the telescope has high counting rates and in general the backgrounds and corrections to the data are small. On the other hand, the decay corrections for the magnet method become rather large at low meson energies. Thus, to a certain extent the two methods tend to complement each other.

The energy at which B reverses sign is found to be 325 Mev as compared to 335 Mev obtained in the magnet experiment. If one assumes a simple resonance theory as Watson[8] has done, one finds that B should pass through zero when

$$[\cos(\alpha_{33}-\alpha_3)+2\cos(\alpha_{33}-\alpha_1)]=0, \qquad (6)$$

where α_{33}, α_3, and α_1, are the phase-shifts obtained in the analysis of meson scattering experiments. If one uses the phase shifts as calculated by Bethe and deHoffmann,[9] the above quantity equals zero at 340 Mev. Thus, these experiments conform quite well to the predictions of this set of phase shifts. A more detailed comparison with the phenomenological theory of Watson and Gell-Mann[8] is in preparation and will be published at a later date.

ACKNOWLEDGMENTS

The authors wish to acknowledge the help and support received from all members of the synchrotron laboratory during the progress of this experiment. We are indebted particularly to Dr. R. F. Bacher. Also, Dr. R. V. Langmuir, Dr. J. G. Teasdale, Dr. R. L. Walker, Dr. D. C. Oakley, and Mr. B. H. Rule assisted in running the machine.

[8] K. M. Watson, lectures at CalTech during the summer of 1954; M. Gell-Mann and K. M. Watson, Ann. Rev. Nuc. Sci. 4, 219 (1954).

[9] H. A. Bethe and F. deHoffmann, Phys. Rev. **95**, 1100 (1954).